Tests of hadronic interaction models by data of the KASCADE-Grande air-shower experiment

A. Haungs, M. Risse, W.D. Apel, F. Badea, K. Bekk, J. Blümer, H. Bozdog, K. Daumiller, P. Doll, R. Engel, J. Engler, H.J. Gils, D. Heck, J.R. Hörandel, T. Huege, H.O. Klages, G. Maier, H.J. Mathes, H.J. Mayer, J. Milke, M. Müller, S. Nehls, R. Obenland, J. Oehlschläger, S. Ostapchenko, T. Pierog, S. Plewnia, H. Rebel, M. Roth, H. Schieler, M. Stümpert, H. Ulrich, J. van Buren, A. Weindl, J. Wochele

Institut für Kernphysik, Forschungszentrum Karlsruhe, and Institut für Experimentelle Kernphysik, Universität Karlsruhe, 76021 Karlsruhe, Germany

A. Bercuci, I.M. Brancus, B. Mitrica, M. Petcu, O. Sima, G. Toma

National Institute of Physics and Nuclear Engineering, 7690 Bucharest, Romania

M. Bertaina, A. Chiavassa, F. Di Pierro, P.L. Ghia, C. Morello, G. Navarra, G.C. Trinchero

Dipartimento di Fisica Generale dell'Università, and Istituto di Fisica dello Spazio Interplanetario, INAF, 10125 Torino, Italy

M. Brüggemann, P. Buchholz, C. Grupen, Y. Kolotaev, S. Over, W. Walkowiak, D. Zimmermann

Fachbereich Physik, Universität Siegen, 57068 Siegen, Germany

R. Glasstetter, K.-H. Kampert

Fachbereich Physik, Universität Wuppertal, 42097 Wuppertal, Germany

A. Risse, J. Zabierowski

Soltan Institute for Nuclear Studies, 90950 Lodz, Poland

Received Nov 30, 2005

KASCADE-Grande is a multi-detector setup to get redundant information on single air shower basis. The information is used to perform multi-parameter analyses to solve the threefold problem of the reconstruction of the unknown primary energy, the primary mass, and to quantify the characteristics of the hadronic interactions in the air-shower development. This contribution discusses the various ways of testing the hadronic interaction mechanisms with data of the original KASCADE experiment and their results, as well as the capabilities in testing the models with the extension of KASCADE, the KASCADE-Grande experiment. Though no hadronic interaction model is fully able to describe the multi-parameter data of KASCADE consistently, the more recent models or improved versions of older models reproduce the data better than a few years ago.

PACS: 96.50.sd
Key words: cosmic rays, extensive air showers, hadronic interactions

1 Introduction

The all-particle energy spectrum of cosmic rays shows a distinctive feature at a few PeV, known as the knee, where the spectral index changes from -2.7 to approximately -3.1 (Fig. 1). At that energy direct measurements are presently not possible due to the low flux, but indirect measurements observing extensive air showers (EAS) are performed.

Despite EAS measurements with many experimental setups in the last five decades the origin of the kink is still not clear, as the disentanglement of the threefold problem of estimate of energy and mass plus the understanding of the air-shower development in the Earth's atmosphere remains an experimental challenge [1].

There are various measuring techniques for air showers, but all interpretations of the measured observables in terms of primary energy and mass require a good knowledge of the shower development in the atmosphere and of the interaction mechanisms of high-energy particles with air nuclei. Extensive Monte Carlo simulation procedures are used as reference patterns. For the high-energy hadronic interactions more or less bold extrapolations from lower energies, formulated as theoretical models and parameterizations, are at disposal. For example, at the knee energies accelerator data are still not yet available (though the Tevatron collider is close to these energies) either for relevant target projectile combinations or for the kinematic region of secondaries scattered in the extreme forward direction. This situation leads to an uncertainty of unknown order, in some sense only to be guessed by using the same reconstruction procedures but different hadronic interaction models. And, it remains unclear if there are common systematic uncertainties in the interaction models by unknown features and interaction paths, not yet taken into account.

The hadronic interaction models used for the interpretation of air shower data are embedded in Monte Carlo simulation programs like CORSIKA [4]. They are based on parton-parton interactions and approaches, inspired by QCD, considering the lowest-order interaction graphs involving the elementary constituents of hadrons (quarks and gluons). However, there are not yet exact ways to calculate the bulk of soft processes since for small momentum transfer the coupling constant α_s of the strong interaction is so large that perturbative QCD fails. Thus we have to rely on phenomenological models which incorporate concepts of scattering theory. Models like SIBYLL [5, 6] or QGSJET [7], describe particle production by exchange of one or multiple Pomerons. Inelastic reactions are simulated by cutting Pomerons, finally producing two colour strings per Pomeron which subsequently fragment into colour neutral hadrons. Differences between the models arise from the particular implementation of the Pomeron concept and string fragmentation. Crucial parameters in the modeling of hadronic interaction models are the total nucleus-air cross-section and the parts of the inelastic and diffractive cross sections leading to shifts of the position of the shower maximum in the atmosphere, and therefore to the particle numbers (muons, electrons, hadrons) as well as to their correlations on single air shower basis. The multiplicity of the pion generation as

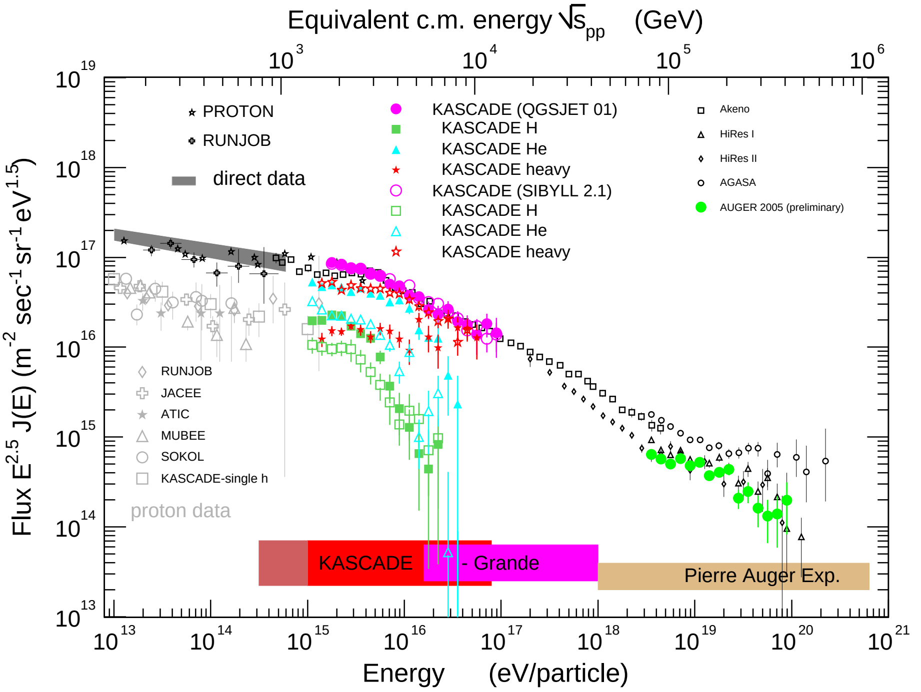

Fig. 1. Primary cosmic ray flux and primary energy range covered by KASCADE and its extension KASCADE-Grande. The results of KASCADE [2] are also included, as well as the preliminary results of the Pierre Auger Experiment [3].

well as their p_t-distribution at all energies at the hadronic interactions during the air shower development are also 'semi-free' parameters in the air-shower modeling as accelerator data have still large uncertainties.

The simulation package CORSIKA is based on three program parts: High energy interaction models as discussed above, low energy interaction models, like FLUKA [8] or GHEISHA [9], and the package EGS4 [10] which is responsible for the electromagnetic processes during the shower development. The low-energy models are used below a certain interaction energy which is a free parameter in CORSIKA. For KASCADE simulations the transition energy is chosen to 80 GeV for GHEISHA, and 200 Gev for FLUKA, respectively. CORSIKA itself provides the frame for these models and handles the transport of the particles through the atmosphere.

Due to the phenomenological character of the models data are needed to tune the free parameters and to verify or to falsify theoretical assumptions of the models.

The multi-detector system KASCADE-Grande (KArlsruhe Shower Core and Array DEtector) [11] approaches the problems of interpreting the air showers by measuring as much as possible complementary information from each single shower event. The multi-detector arrangement allows to measure the total electron and muon numbers of the shower separately using an array of shielded and unshielded detectors at the same place. Furthermore, local muon densities are being measured at three additional threshold energies and the hadronic core of the showers with an iron sampling calorimeter. All these information are also available for measurements with the Grande array, which is an extension of KASCADE by factor 10 in area and accessible primary energy [12, 13]. KASCADE-Grande has started its regular measurements at the end of 2003, hence, no results can be presented from that part, but the capabilities for testing models will be shown. Recently, an array of dipole antennas were additionally set up at the KASCADE-Grande site for a coincident observation of particles on ground with the radio signal emitted during the shower development by interactions of the charged particles with the Earth's magnetic field [14].

In a separate contribution to this conference the main results of KASCADE, in particular the reconstruction of energy spectra of single primary mass groups are discussed [2, 15]. There, it is shown that the quality of the data allows to unfold the 2-dimensional electron number - muon number shower size spectrum in energy spectra of single mass groups. The results can be summarized by the conclusive evidence that the knee is caused by a suddenly appearing strong decrease of the flux of light primaries, where the knee positions show a dependence on the primary mass group. Systematic uncertainties for the estimate of the elemental composition are dominated by the inadequacy of the hadronic interaction models underlying the reconstruction of energy spectra of single mass groups.

In this contribution approaches of further correlation analyses to test the hadronic interaction models and to find constraints for the improvement and development of the next generation of the models are presented. These tests provide complementary information to the data of present accelerator experiments, as air-shower data are sensitive to higher energy interactions and to a different (extreme forward direction) kinematic region.

2 The KASCADE-Grande experiment

The KASCADE experiment [11] measures showers in a primary energy range from 100 TeV to 80 PeV and provides multi-parameter measurements on a large number of observables including electrons, muons at 4 energy thresholds, and hadrons. The main detector components of KASCADE are the Field Array, the Central Detector, and the Muon Tracking Detector (Fig. 2).

The Field Array measures the total electron and muon numbers ($E_\mu > 230\,\mathrm{MeV}$) of the shower separately using an array of 252 detector stations containing shielded and unshielded detectors at the same place in a grid of $200 \times 200\,\mathrm{m}^2$. The excellent time resolution of these detectors allows also good determination of the arrival directions of the showers.

The Muon Tracking Detector measures the incidence angles of muons ($E_\mu >$

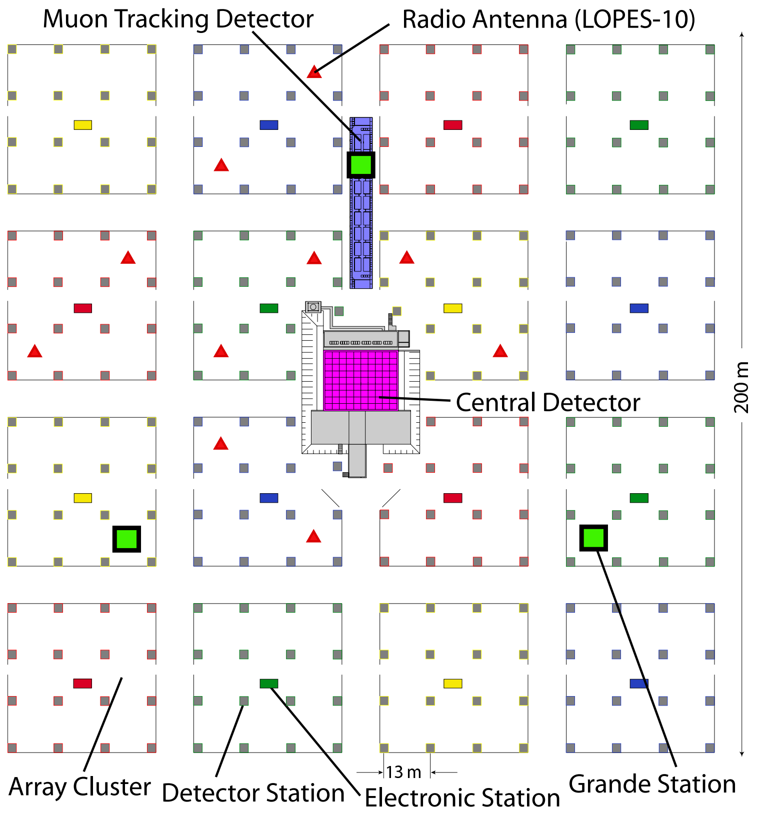

Fig. 2. The main detector components of the KASCADE experiment: (the 16 clusters of) Field Array, Muon Tracking Detector and Central Detector. The location of some stations of the Grande array as well as the positions of 10 LOPES dipole antennas are also displayed.

800 MeV) relative to the shower arrival direction.

The hadronic core of the shower is measured by a 300 m^2 iron sampling calorimeter installed at the KASCADE Central Detector. The calorimeter is equipped with 11 000 warm-liquid ionization chambers in nine layers [16]. Due to the fine segmentation (25×25 cm^2) energy, position, and angle of incidence can be measured for individual hadrons ($E_\mathrm{h} > 50$ GeV).

Three other components at the Central Detector - trigger plane (serves also as timing facility), multiwire proportional chambers (MWPC), and limited streamer tubes (LST) - offer additional valuable information on the penetrating muonic component at 490 MeV and 2.4 GeV energy thresholds.

The multi-detector concept of the KASCADE experiment which is operating since 1996 has been translated to higher primary energies through KASCADE-

Grande [12]. The 37 stations of the Grande array extend the cosmic ray measurements up to primary energies of 1 EeV. The Grande stations, 10 m^2 of plastic scintillator detectors each, are spaced approximatively by 130 m covering a total area of ~ 0.5 km^2 including the original KASCADE array in the north-east corner of Grande.

For the calibration of the radio signal emitted by the air shower in the atmosphere an array of first 10 and meanwhile 30 dipole antennas (LOPES) is set up on the site of the KASCADE-Grande experiment [17].

3 Tests with electron number - muon number correlations

Comparing the unfolding results (see [2, 15] and Fig. 1) based on the two different hadronic interaction models, the model dependence when interpreting the data is obvious, especially for the relative abundances of the different mass groups. Modeling the hadronic interactions underlies assumptions from particle physics theory and extrapolations resulting in large uncertainties, which are reflected by the discrepancies of the results presented here. The most prominent difference lies in the larger contribution of heavier primaries in case of the SIBYLL model, especially at high energies. To understand the differences between the results based on the two different models and to judge the validity of the models in general detailed investigations of the results are performed. In Fig. 3 the predictions of the N_e and N_μ^{tr} correlation for the two models are given in case of proton and iron primaries. It is remarkable that all four lines have a more or less parallel slope which is different from the data distribution. There, the knee is visible as kink to a flatter N_e-N_μ^{tr} dependence above $N_\mu^{tr} \approx 4.2$. The heavier primary contribution to the results based on the SIBYLL model is due to predictions of a larger ratio of electron to muon number for all primaries. Comparing the residuals of the unfolded two-dimensional distributions for the different models with the initial data set we conclude [15] that at lower energies the SIBYLL model and at higher energies the QGSJET model are able to describe the correlation consistently, but none of the present models gives a contenting description of the whole data set. Also preliminary analyses [18] using the FLUKA [8] code instead of GHEISHA [9] as low energy interaction model or using the new model QGSJet II [19] as high energy interaction model show no conspicuous improvement of the situation.

4 Tests with hadronic observables

Arbitrary changes of free parameters in the interaction models will change the correlation of all shower parameters. Tests using KASCADE observables, which are measured independently of such used in the unfolding procedure, may give further constraints, e.g. by investigating correlations of the hadronic shower component with electron or muon numbers. The aim is to provide hints for the phenomenology physicists who develop the models how the parameters (and the theory) should be modified in order to describe all the data consistently.

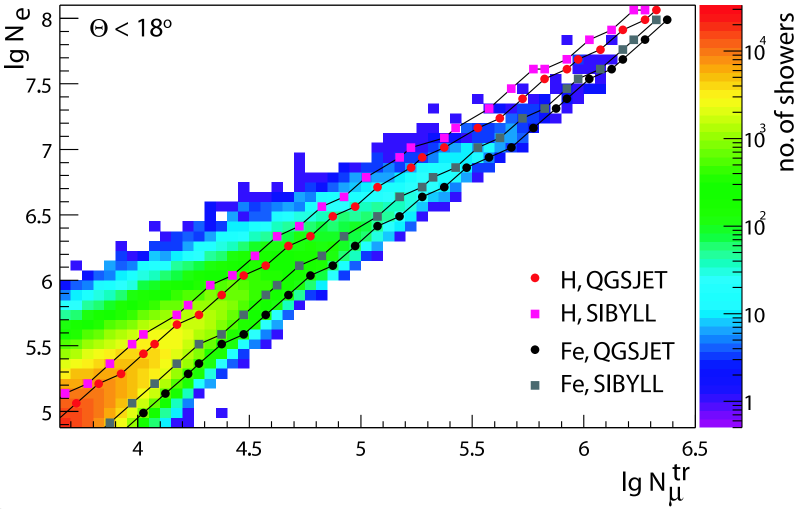

Fig. 3. Two-dimensional electron (N_e) vs. muon (N_μ^{tr} = number of muons in 40-200m core distance) number spectrum measured by the KASCADE array. The lines display the most probable values for proton and iron primaries obtained by CORSIKA simulations employing different hadronic interaction models.

The first applied method is to evaluate the measured data relative to simulations (including the detector response) of proton and iron primaries. The measurements have to lie between these extreme values, otherwise the simulations cannot describe this specific observable correlation. An example of such a correlation is shown in Fig. 4. Direct comparisons between data and simulations are not possible due to the unknown composition of the primary particles generating the air showers.

These kinds of tests are performed for a large set of interaction models employed in the simulation package CORSIKA [4]. In ref. [20] first results of these tests were published investigating the models VENUS 4.12 [21], SIBYLL 1.6 [5], and QGSJET 98 [7]. The general conclusion was that QGSJET described the data best at that time, whereas strong hints could be given that SIBYLL 1.6 generates too few muons. These results triggered improvements of the model leading to the newer version SIBYLL 2.1 [6]. Later [22], NEXUS 2 [24], SIBYLL 2.1 and QGSJET 01 [23] were investigated with the result that the differences between the models got smaller. Whereas QGSJET 01 and SIBYLL 2.1 can now describe the KASCADE hadronic observables, NEXUS calculations predict in respect to the number of electrons too little hadronic energy at the observation level. Present investigations comparing the data with DPMJET 2.55 [25], QGSJET 01, and SIBYLL 2.1 confirm that these three models can describe the hadronic observables and their correlations with the electron and muon component within the sensitivity of the KASCADE experiment (Fig. 4), at least in the energy range below 10 PeV.

For a more detailed test of the interaction models by hadronic data the un-

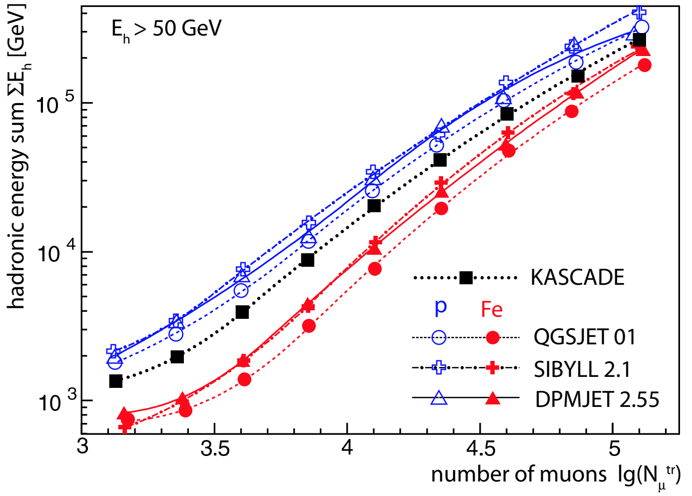

Fig. 4. Correlation between the reconstructed hadronic energy sum and the number of muons. Predictions from detailed simulations for different models and primary proton and iron nuclei are compared with KASCADE data.

known mass composition clouding direct comparisons is disentangled, for which the following approach is chosen [26]: The compositions determined by the unfolding of the two-dimensional lg N_e-lg N_μ^tr spectrum for the specific models are used to check, if these models can describe the hadronic observables. For example correlations of hadron number and muon number predicted for the simulation using QGSJET/GHEISHA including the mass composition resulting from [15] show a disagreement with data at lower energies, but a good agreement at higher energies. The situation for SIBYLL/GHEISHA is opposite. While for smaller primary energies the hadronic observables as well as the electron-muon data are reproduced rather well, there are discrepancies at higher energies. These findings are compatible with the consistency checks done with electron number vs. muon number correlations alone [2, 15].

Further tests using the hadronic data of KASCADE are envisaged, e.g. by following approach: The change of specific parameters in one certain model (QGSJET 01) with an investigation of the change of the correlations of measurable observables [27, 28] and a following comparison with the data. These specific changes concerns the proton-air cross section (inside the uncertainties given by experimental values, e.g. by HiRes [29]) or the inelasticity coefficient of the interaction (an increase by about 10% to 15%, which is also inside the uncertainty given by the models). Indeed, such modifications lead to significant changes in the particle numbers at ground level. But for a complete picture the correlations between all shower components have to be analyzed in more detail.

A different window to check the hadron-muon correlation predicted by shower simulations is the investigation of the KASCADE trigger rates [30]. Here, in particular primaries of lower energies and their behavior in the atmosphere is approached. By this, indications for an underestimate of the non-diffractive inelastic cross-section in the models are given.

5 Tests by analysing the geometric structure of the hadronic shower core

In another analysis of the KASCADE hadronic data, with the geometric structure of jet production in ultra high energy hadronic interactions a special interaction feature is tested more directly. Here, the geometric distribution of high-energy hadrons $\geq$100 GeV in shower cores measured with the KASCADE calorimeter is studied [31]. Geometric structures in hadronic shower cores at observation level are particularly interesting, as one expects QCD jet production to lead to secondary hadrons being naturally aligned to form line shape patterns [32]. Similar alignment structures might result from exotic hadron production processes [33]. Aligned event structures were, for instance, reported by the PAMIR experiment [34, 35, 36].

For the KASCADE analysis, showers above 10^{15} eV were selected, with the shower core well contained in the central calorimeter. At least four hadrons above 100 GeV are required, and two observables are constructed from the geometric position of the four highest-energy hadrons: λ_4, a parameter commonly used in the

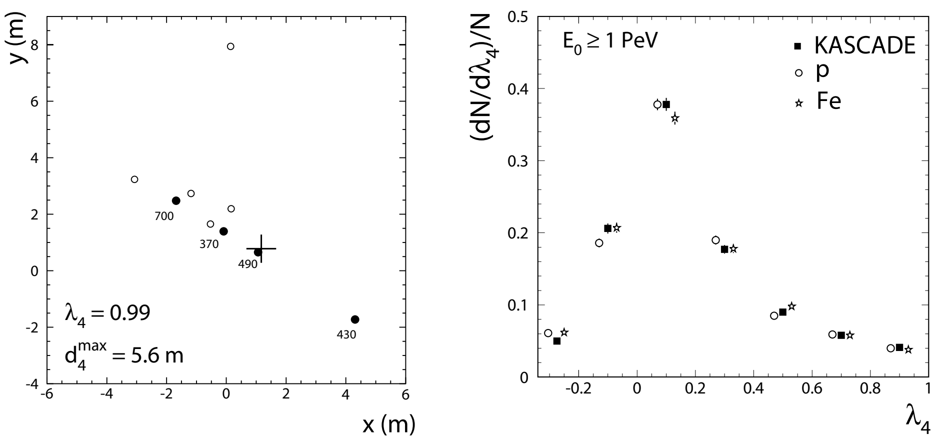

Fig. 5. Left: Example of a measured hadronic shower core (hadron positions in the shower plane) with $\lambda_4 = 0.99$ and $d_4^{\max} = 5.6$ m. 9 hadrons with energies above 100 GeV are reconstructed. For the four most energetic hadrons (full symbols), the energies in GeV are given. The shower core position as reconstructed by the scintillator array is marked by a cross. The active calorimeter area exceeds the area plotted. Right: λ_4 distribution measured by KASCADE compared to simulation results for primary proton and iron showers. For clarity, simulation points are slightly displaced horizontally.

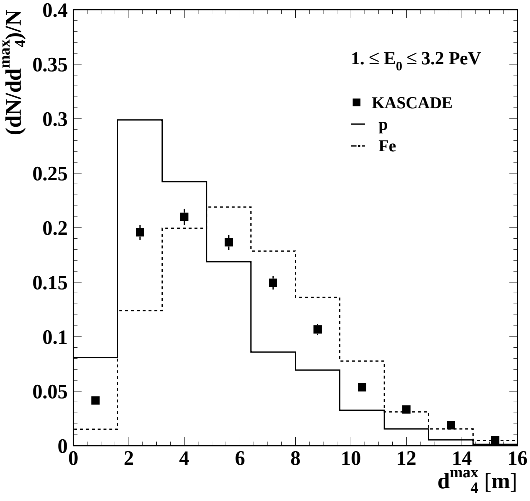

Fig. 6. $d_4^{\max}$ distribution measured by KASCADE compared to simulation results for primary proton and iron showers for primary energies of 1-3.2 PeV.

past to quantify the angular correlation of particles [37], with values ranging from $-1/3$ for an isotropic to 1 for a perfectly aligned event topology; and $d_4^{\max}$, the maximum distance between one of the four hadrons to the geometric centre of the other three [39]. An example of a measured event showing alignment is given in Fig. 5, left. Usually, events are termed "aligned" for $\lambda_4 \geq 0.8$.

The measured λ_4 distribution is displayed in the right panel of Fig. 5. The data set comprises 4489 events. Also shown are the results for primary proton and iron nuclei simulated with the CORSIKA (v6.0) code [4] employing the QGSJET 01 [7, 23] hadronic interaction model. The measured λ_4 distribution and the fraction of aligned events of high-energy hadrons are well reproduced by the standard simulations. Increasing the primary energy threshold of 10^{15} eV, also no dependence on the shower energy was observed. In a detailed simulation study, e.g. by artificially increasing the transverse momentum p_t of secondary hadrons, no correlation between λ_4 and hadronic interaction features such as jet production was found. Moreover, it was shown that the data can be reproduced based on randomly distributed hadron azimuth angles. Comparing the KASCADE to PAMIR data, both λ_4 distributions were found to resemble each other very well, in spite of the different observing conditions.

The other geometric observable investigated, the parameter $d_4^{\max}$, turned out to be sensitive to the primary particle type and to the transverse momentum values assumed in high-energy hadron interactions. The $d_4^{\max}$ distribution measured by KASCADE is compared to simulations in Fig. 6. The KASCADE data are mostly

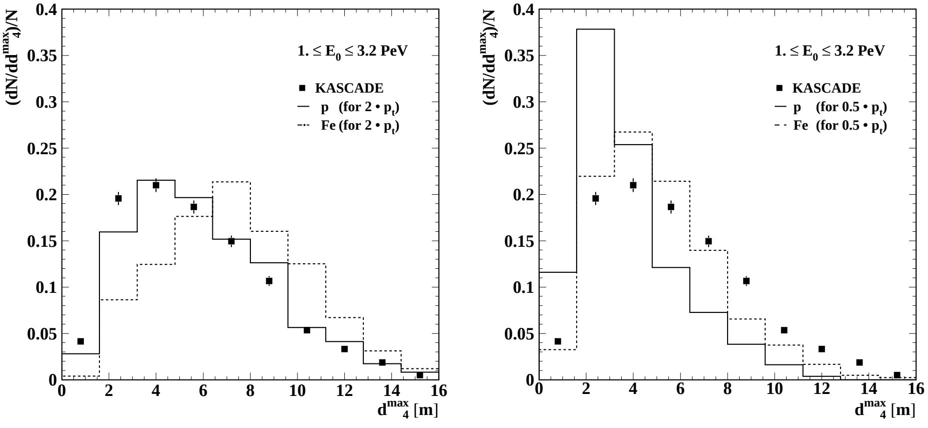

Fig. 7. $d_4^{\max}$ distribution measured by KASCADE (see Fig. 6) compared to simulation results for primary proton and iron showers with modified transverse momentum of secondary hadrons. The transverse momenta were artificially increased (left panel, "$2 \cdot p_t$") and reduced (right panel, "$0.5 \cdot p_t$") by a factor two.

bracketed by the primary proton and iron expectations which seems reasonable for primary energies below the knee. Assuming transverse momenta of secondary hadrons produced in high-energy interactions twice as large as in standard simulations (left panel in Fig. 7), the distributions both for proton and iron primaries are significantly shifted to larger $d_4^{\max}$ values. In this scenario, the simulations are hardly able to provide a satisfactory description of the $d_4^{\max}$ data. The same conclusion holds when artificially reducing the p_t of secondary hadrons by a factor two (right panel in Fig. 7). Therefore, hypothetical transverse momenta in high-energy secondary hadron production that differ by a factor two or more from the standard assumptions are disfavored by the KASCADE data.

6 Tests with muon densities

In this section we endeavor to analyze local muon densities in air showers for three different muon energy thresholds. Therewith, the consistency of the simulations with respect to the muon energy spectrum and systematic features of different Monte Carlo models can be revealed. The ratio of muon densities measured at fixed core distances are determined by the muon energy spectrum in air-showers, which is a different approach to test the models than investigating the total number of muons [40].

At KASCADE, local muon densities of single air showers are measured for three muon energy thresholds by separate detector set-ups. Two of them are installed at the Central Detector which is placed in the geometrical center of the KASCADE

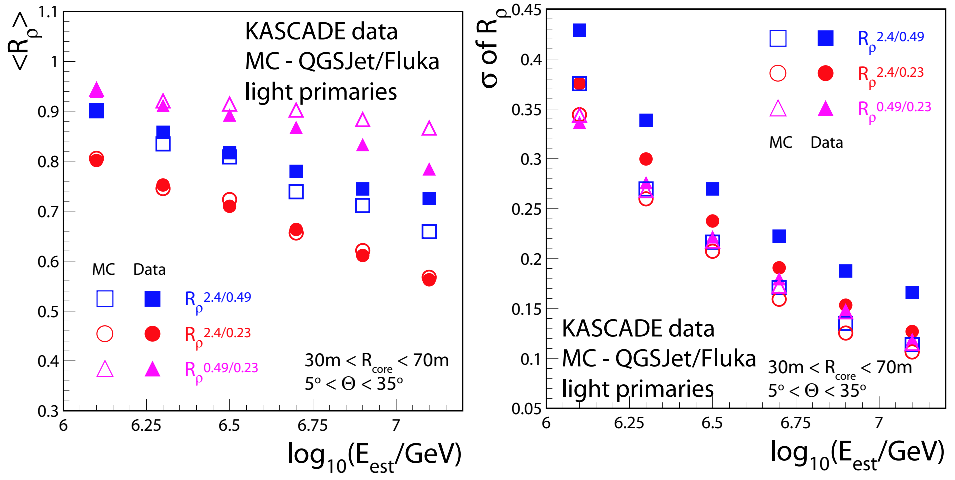

Fig. 8. Mean and width of the muon density ratio distributions R_ρ vs. primary energy for measurements and simulations using QGSJet/FLUKA.

detector array. A setup of 32 large multiwire proportional chambers (MWPC) is installed in the basement of the building and enables the estimation of the muon density $\rho_\mu^{2.40GeV}$ for each single EAS. The total absorber corresponds to a threshold for muons of 2.4 GeV kinetic energy. The second muon detection system is a layer of 456 plastic scintillation detectors in the third gap of the Central Detector, called trigger plane. Here the muon density $\rho_\mu^{0.49GeV}$ is estimated for muons with a threshold of 490 MeV for vertical incidence. The third local muon density is reconstructed with help of the KASCADE array data. 196 detector stations contain shielded plastic scintillators which are used to reconstruct the total muon number of the showers by fitting the lateral distributions. For the present analyses this LDF is used to estimate the densities of muons at the place of the central detector ($\rho_\mu^{0.23GeV}$). The primary energy of the showers is roughly estimated by a combination of reconstructed shower sizes determined by data of the KASCADE array. In the present analysis, the total sample of measured events is further divided in 'electron-rich' (induced by light primaries) and 'electron-poor' (induced by heavy primaries) showers performed by a cut along the ratio $lg(N_\mu)/lg(N_e)$, i.e. observables estimated by the arrays data only.

The ratios $R_\rho^{2.4/0.49} = \rho_\mu^{2.40GeV}/\rho_\mu^{0.49Gev}$, $R_\rho^{2.4/0.23} = \rho_\mu^{2.40GeV}/\rho_\mu^{0.23Gev}$, and $R_\rho^{0.49/0.23} = \rho_\mu^{0.49GeV}/\rho_\mu^{0.23Gev}$ are the relevant parameters for the present analysis. Using KASCADE data the analysis is concentrated to showers in the core distance of $30 - 70$ m, requiring primary energy above 10^{15} eV. A large set of CORSIKA simulations have been performed using different interaction models, e.g. QGSJet (vers. of 1998) or SIBYLL (vers.2.1), for the high-energy interactions and GHEISHA and FLUKA for low-energy interactions. Observation level, Earth's magnetic field, and the particle thresholds are chosen in accordance with the experimental situation of KASCADE-Grande as well as the simulation of the detector responses.

Fig. 8 shows the dependence of the mean and fluctuations (width of distributions) of the three considered density ratios on the primary energy for data and predictions by the model combination QGSJET/FLUKA analyzed by same procedures. The general behavior of decreasing mean and fluctuation with increasing energy is reproduced by the simulations, but a clear deviation on the mean values and on the amount of fluctuations is visible. QGSJet/FLUKA are in agreement with the data for low energies and for the full energy range in the ratio $R_\rho^{2.4/0.23}$, which is not the case for other model combinations. For the other two ratio parameters $R_\rho^{2.4/0.49}$, $R_\rho^{0.49/0.23}$ and, especially for the amount on predicted fluctuations there is a general deviation from the data. Other interaction model combinations (e.g. Sibyll/GHEISHA) show a similar behavior, but the disagreement is smallest for the Fluka model.

At KASCADE-Grande [41] similar measurements can be performed for EAS of primary energies at least up to 10^{17} eV. The muon detection at the KASCADE central detector will then be possible for core distances of $50-550$m with reasonable muon statistics. This test of the validity of the muon component will be of high relevance for the shower simulation procedures at ultra-high energies.

7 Tests of muon pseudorapidities

Another approach to test the hadronic interaction models via the muon component is possible due to the excellent angular resolution of the KASCADE Muon Tracking Detector (≈0.35°). Measuring the relative angles τ and ρ between single shower muons and the shower axis the pseudorapidity $\eta = ln\frac{2p_\parallel}{p_t} \approx -ln(\sqrt{\tau^2+\rho^2}/2)$ can be calculated. Fig. 9 shows the correlation of the pseudorapidity of the muons measurable in the detector and of their parent hadrons [42, 43]. The rapidity distribution of hadrons generated in high-energy hadronic interactions is still an open question and an important parameter for the model building.

In Fig. 9, right panel, the distribution of the energies of the grandmother hadrons producing muons which can be registered in the muon tracking detector is shown for three collecting distances, where the two subgroups are the distributions relevant for KASCADE and KASCADE-Grande measurements, respectively. The break at 80 GeV, where the change of the interaction model takes place is clearly seen. It is more pronounced in KASCADE setup and indicates that number of muons produced according to high-energy and low-energy interaction models do not match at the boundary energy.

These simulation results show the sensitivity of muon measurements with a high angular resolution to the features of the hadronic interaction models. Due to the larger distances the analysis of these measurements are more promising in case of KASCADE-Grande than for KASCADE data.

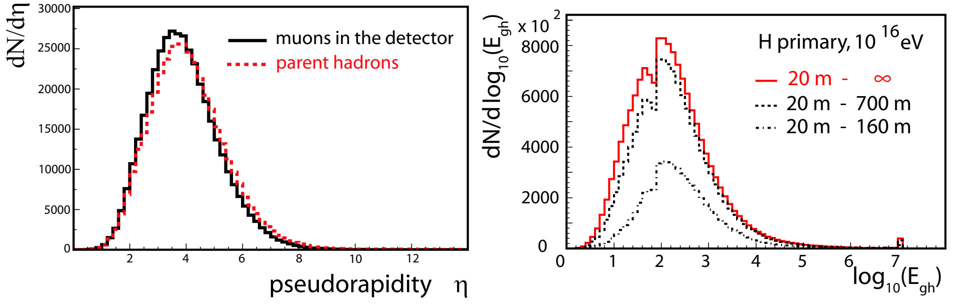

Fig. 9. Left: Pseudorapidity distribution predicted by CORSIKA/QGSJET simulations for muons detectable in KASCADE and for the parent hadrons of the same muons. Right: Distribution of "grandmother" hadron energies, i.e. the interaction energy, which produce a pion or kaon which decay into a muon reaching the ground level. Note the break at 80 GeV, where the interaction models change.

8 Test of the electromagnetic processes in the shower development

Lateral distributions for electrons in extensive air showers measured with the array of the KASCADE experiment are compared to results of simulations based on the high-energy hadronic interaction models QGSJet and SIBYLL. The relevant parameter, commonly used to describe the form of the lateral density distribution, is the lateral form parameter in the Nishimura-Kamata-Greisen (NKG)-function, usually called age [44]. The name expresses the relation between the lateral shape of the electron distribution and the height of the shower maximum. Due to the statistical nature of the shower development, the height of the shower maximum is subject to strong fluctuations. Showers, which have started high in the atmosphere show a flat lateral electron distribution, as electrons in the electromagnetic cascade suffer more from multiple scattering processes. Such showers are called old and are characterised by a large value of the age parameter. Young showers have started deeper in the atmosphere and had their maximum more close to observation level. This results in a steeper lateral electron distribution, which corresponds to a smaller value of the shape parameter. Apart from fluctuations, the height of the shower maximum depends on energy and mass of the shower initiating primary. Therefore, the lateral shape parameter is also sensitive to the mass of the primary.

The relations of primary energy with the shape parameter s and with the primary mass are illustrated in Fig. 10. Here, the energy is given by an estimator $\varepsilon_{\lg E}$, which is obtained from simulations by a simple relation of the $\lg N_\mu - \lg N_e-$ system. The shape parameter is obtained by fitting a modified NKG-function to the measured lateral distributions on a single air shower basis [44]. The shape parameter as a function of this energy estimator $\varepsilon_{\lg E}$ is shown for both, data and Monte Carlo simulations of all five elements. It is obvious, that showers from light primaries are younger in average, i.e. have smaller shape values compared to heavy primaries, and showers of high energy are younger than low energy ones.

Compared with QGSJet simulated showers (Fig. 10, upper panel), the data fit into this picture only qualitatively. Up to an energy of about 10 PeV, they follow the line of carbon. For higher energies, the lateral shape parameter stays almost constant and crosses the line of iron at an energy of about 30 PeV. Beyond this crossing point, the absolute values of the measured shape parameter cannot be explained by any elemental composition within this Monte Carlo model.

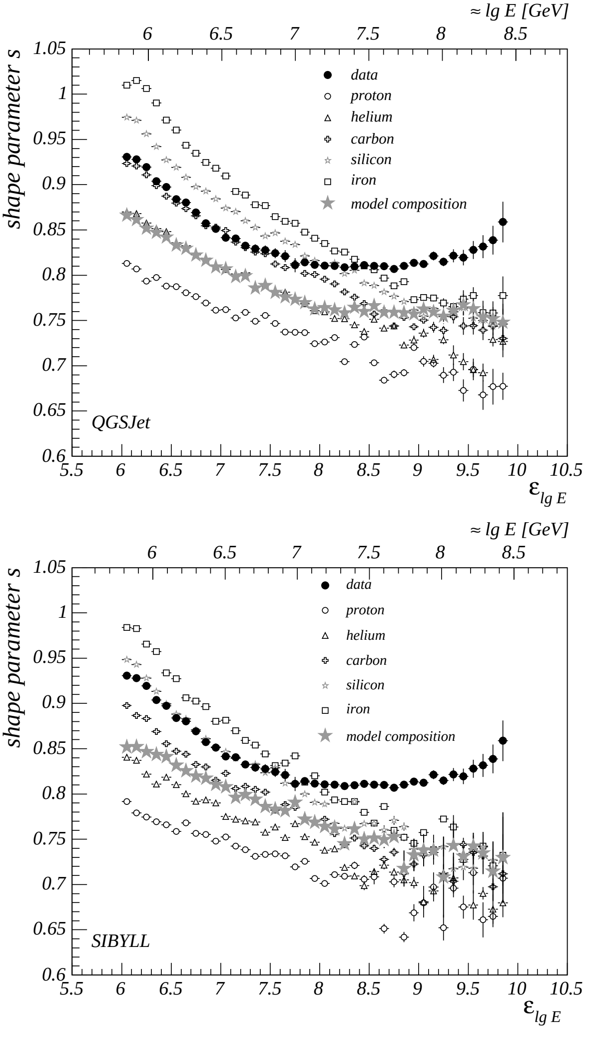

Fig. 10. Reconstructed shape parameter as a function of the energy estimator $\varepsilon_{\lg E}$ for KASCADE data, five primary masses and a model composition as simulated using QGSJet (top) and SIBYLL (bottom). The scale on top gives a rough estimate for $\lg E$ in GeV.

For a more detailed investigation the data distributions are compared with what would be expected from the simulations, once a reasonable elemental composition is given. For this, the simulated shower events of the five elemental masses have been weighted with individual energy spectra, which have been reconstructed from an analysis of the measured N_e/N_μ-spectrum using a sophisticated unfolding algorithm based on the same model QGSJet. The resulting composition favors light elements before the knee and a significant contribution from heavy elements at energies above the knee [2]. The effect on the shape parameter of the sum of these simulated showers as a function of the energy estimator is also shown in Figure 10. It is remarkable, that the line of the measured shape parameter values runs almost parallel to the line representing these adapted Monte Carlo predictions, but is displaced by a nearly constant amount of $\Delta s \sim 0.05$ over the whole energy range.

The almost constant value of the shape parameter for energies beyond 10 PeV can be understood as the result of a transition from light to heavy nuclei in the elemental composition of cosmic rays. The offset between the lines of measured and simulated shape simply states, that the simulations in general yield slightly steeper shapes than observed in real showers.

The data have also been compared with simulations based on the SIBYLL model (Fig. 10, bottom panel). The SIBYLL calculated shapes predict a more heavy composition, as a result of small differences in the e/μ-ratios. In addition, the mean lateral electron distributions appear a bit younger. SIBYLL describes the data worse compared to QGSJet. The SIBYLL iron curve crosses the data already at an energy of about 10 PeV, so there is no explanation for the measured shape values within this model for larger energies. Comparing with QGSJet one finds that the mean shape of SIBYLL showers in general is smaller by $\Delta s \sim 0.05$.

Summarizing, both models are not able to describe the measured lateral distribution of the e/γ-component correctly. The details of the form of the lateral distribution depend on the hadronic interaction mechanism as well as on electromagnetic cascading processes. Thus, a variant of the QGSJet model that predicts a larger e/μ-ratio, would give better consistency with data. However, the discrepancies might also be buried in the electromagnetic cascading algorithm EGS4 and its treatment of the multiple coulomb scattering process.

9 Tests of the shower development

Investigating further shower observables at KASCADE like the muon arrival time distributions [45], the electron and muon lateral distributions or the muon production heights [46] enable to scrutinize the shower development itself rather than the hadronic interactions. In summary, within the given sensitivity of KASCADE CORSIKA describes the shower development reasonably well and no significant deviations were found.

10 Summary

Measurements with the multi-detector setup KASCADE provide plenty of high quality data to investigate the physics of the knee in the cosmic ray energy spectrum. Concerning the main task of the experiment, the reconstruction of energy spectra of elemental mass groups, conclusive evidence has been given that the knee is caused by a suddenly appearing strong decrease of the flux of light primaries, where the knee positions show a dependence on the primary mass group. Systematic uncertainties for the estimate of the elemental composition are dominated by the inadequacy of the hadronic interaction models underlying the unfolding analysis.

Further indications for the inadequate description of the hadronic interactions in the atmosphere are given by additional KASCADE data analyses taking the advantage of the multi-detector information, i.e. investigations of the hadron component in air-showers or of muon properties measured for different muon energy thresholds. These investigations of observable correlations have shown that none of the present hadronic interaction models is able to describe all the KASCADE data consistently (on a level of a few percent), and, by the different analysis with KASCADE data hints for the inadequacy were found for the high energy interaction models, for the low energy interactions models, as well as possibly for the description of the electromagnetic processes in the shower development.

The tests will be continued with new models, e.g. QGSJET II [19], and with better statistical accuracy at higher primary energies. But, the same analyses will be performed also for showers where the global parameters are estimated with help of the Grande array. Grande measures in coincidence with KASCADE since the end of the year 2003, and the same kind of analyses will be performed at KASCADE-Grande [12, 13] at least up to a few times 10^{17} eV. Especially the unfolding procedures of the two-dimensional shower size spectrum with the following investigations and tests of the validity of the hadronic interaction models and all the described tests using the information from the different muon detection facilities of KASCADE-Grande will be possible.

Recently, some efforts were made to sample the information from accelerator experiments and cosmic ray investigations [47] to improve the hadronic interaction models. In future, by having the data of the KASCADE-Grande experiment and by further improving the hadronic interaction models better constraints especially at higher primary energies are expected. Then, these tests of the validity of the air shower simulation tools will be of high relevance for the shower reconstruction at ultra-high energies.

KASCADE-Grande is supported by the Ministry for Research and Education of Germany, the INFN of Italy, the Polish Ministry of Science and Information Society Technologies (grant for 2004-06), and the Romanian National Academy for Science, Research and Technology.

References

[1] A. Haungs, H. Rebel, and M. Roth, Rep. Prog. Phys. **66** (2003) 1145.

[2] H. Ulrich et al. - KASCADE Collaboration, these proceedings

[3] P. Sommers for the Pierre Auger Experiment, 29^{th}ICRC (Pune) HE1.5 (2005).

[4] D. Heck et al., Report FZKA **6019**, Forschungszentrum Karlsruhe (1998).

[5] J. Engel et al., Phys. Rev. D **46** (1992) 5013.

[6] R. Engel et al., 26^{th}ICRC (Salt Lake City) 1 (1999) p.415.

[7] N.N. Kalmykov, S.S. Ostapchenko, Phys. Atom. Nucl. **56** (1993) 346.

[8] A. Fassò et al., Proc. 'Monte Carlo 2000', eds. Kling et al., Springer, Berlin, (2001) 955.

[9] H. Fesefeldt, Report PITHA-85/02, RWTH Aachen (1985).

[10] W.R. Nelson, H. Hiroyama, and D.W.O. Rogers, SLAC Report 265 (1985).

[11] T. Antoni et al. - KASCADE Collaboration, Nucl. Instr. Meth. A **513** (2003) 429.

[12] G. Navarra et al. - KASCADE-Grande Collaboration, Nucl. Instr. Meth. A **518** (2004) 207.

[13] A. Haungs et al. - KASCADE-Grande Collaboration, 28^{th}ICRC (Tsukuba) 2 (2003) p.985.

[14] H. Falcke et al. - LOPES Collaboration, Nature **435** (2005) 313.

[15] T. Antoni et al. - KASCADE Collaboration, Astropart. Phys. **24** (2005) 1.

[16] J. Engler et al., Nucl. Instr. Meth. A **427** (1999) 528.

[17] A. Haungs et al. - LOPES Collaboration, Proc. 22^{nd} Texas Symposium, Stanford, CA, Dec. 2004, eConf **C041213** (2004) 2413.

[18] H. Ulrich et al. - KASCADE Collaboration, 29^{th}ICRC (Pune) HE1.3 (2005).

[19] S.S. Ostapchenko et al., these proceedings

[20] T. Antoni et al. - KASCADE Collaboration, J. Phys. G: Nucl. Part. Phys. **25** (1999) 2161.

[21] K. Werner, Phys. Rep. **232** (1993) 87.

[22] J. Milke et al. - KASCADE Collaboration, Acta Phys. Pol. B **35** (2004) 341.

[23] D. Heck et al. - KASCADE Collaboration, 27^{th}ICRC (Hamburg) 1 (2001) p.233.

[24] H.J. Drescher et al., Phys. Rep. **350** (2001) 93.

[25] J. Ranft, preprint hep-ph/9911213 (1999).

[26] J. Milke et al. - KASCADE-Grande Collaboration, 29^{th}ICRC (Pune) HE1.3 (2005).

[27] J.R. Hörandel et al. - KASCADE-Grande Collaboration, Nucl. Phys. B (Proc. Suppl.) (2005), in press.

[28] J.R Hörandel et al. - KASCADE-Grande Collaboration, 29^{th}ICRC (Pune) HE1.3 (2005).

[29] K. Belov et al., Nucl. Phys. B (Proc. Suppl.) (2005), in press.

[30] T. Antoni et al. - KASCADE Collaboration, J. Phys. G: Nucl. Part. Phys. **27** (2001) 1785.

[31] T. Antoni et al. - KASCADE Collaboration, Phys. Rev. D **71** (2005) 072002.

[32] F. Halzen and D.A. Morris, Phys. Rev. D **42** (1990) 1435.

[33] I. Royzen, Mod. Phys. Lett. A **9** (1994) 3517.

[34] L.T. Baradzei et al., Proceedings of Intern. Symp. on Cosmic Rays and Part. Phys., Tokyo (1984) 136.

[35] A.S. Borisov et al. - PAMIR Collaboration, 22^{nd}ICRC (Dublin) **4** (1991) p.125.

[36] V.V. Kopenkin, A.K. Managadze, I.V. Rabokolskaya, and T.M. Roganova, Phys. Rev. D **52** (1995) 2766.

[37] A.S. Borisov et al. - PAMIR Collaboration, Izv. Akad. Nauk SSSR, ser. fiz. **49** (1985) 1285.

[38] L.T. Baradzei et al. - PAMIR Collaboration, Izv. Akad. Nauk SSSR, ser. fiz. **50** (1986) 2125.

[39] A. Iwan et al. - KASCADE Collaboration, 28^{th}ICRC (Tsukuba) (2003) p.1595.

[40] A. Haungs et al. - KASCADE-Grande Collaboration, 28^{th}ICRC (Tsukuba) 1 (2003) p.37.

[41] A. Haungs et al. - KASCADE-Grande Collaboration, 29^{th}ICRC (Pune) HE1.5 (2005).

[42] J. Zabierowski et al. - KASCADE Collaboration, 28^{th}ICRC (Tsukuba) 1 (2003) p.29.

[43] J. Zabierowski et al. - KASCADE-Grande Collaboration, 29^{th}ICRC (Pune) HE1.3 (2005).

[44] W.D. Apel et al. - KASCADE Collaboration, Astropart. Phys. (2005), in press, preprint astro-ph/0510810.

[45] T. Antoni et al. - KASCADE Collaboration, Astropart. Phys. **18** (2003) 319.

[46] C. Büttner et al. - KASCADE-Grande Collaboration, 28^{th}ICRC (Tsukuba) 1 (2003) p.33.

[47] R. Engel et al., Nucl. Phys. B (Proc. Suppl.) **122** (2003) 437.